Original Research Article

Experimental Study on Mechanical Coupler Splices in Reinforced Concrete Beams Under Cyclic Flexural Loading

ABSTRACT

This study presents an experiment on the utilization of rebar waste as a mechanical coupler splice material on the reinforced concrete beam. The purpose of using rebar waste is to save costs in a construction project. Experiments were conducted with 3 test specimens, which are reinforced concrete beam without coupler splice (B-13NC), reinforced concrete beam with 19 mm diameter coupler splice (B-13C19) and reinforced concrete beam with 22 mm coupler splice with welding (B-13C22W). Each coupler splice was installed in the plastic hinge area of the beam to determine the maximum capability of the coupler splice. Tests were conducted under cyclic flexural loading on the reinforced concrete beam.

The results showed that the 22 mm diameter coupler splice at B-13C22W has almost the same strength as the reinforced concrete beam without coupler splice (B-13NC). However, the 19 mm diameter coupler splice has a significant decrease in strength, which is more than 30% of the strength of the reinforced concrete beam without a coupler splice (B-13NC). This experiment also shows that the utilization of a coupler splice in the reinforced concrete beams results in a decrease in structural ductility.

Keywords: Reinforced Concrete; Coupler; Ductility; Stiffness; Strength.

1. INTRODUCTION

The beam is a structural element that is subjected to forces acting transversely to its axis, resulting in bending moments and shear forces span-wise [1]. As a crucial component of structural frameworks, beams function to channel loads from floor plates to vertical supports such as columns. Typically, beams are cast monolithically with slabs, and structural reinforcement is placed either at the bottom or both at the top and bottom. The primary stresses experienced by beams include compressive and tensile forces, which are attributed to the influences of bending or lateral forces [2].

The main reason for the large amount of rebars waste in a structural project is that there is rebars that are not in accordance with specifications and mistakes in cutting steel rebars[3].

Research has been conducted onmechanical coupler in test specimens of rebar with diameters of 20 mm, 25 mm, and 32 mm. The test outcomes suggest that the application of

mechanical coupler spliceexhibits a strength comparable to uninterrupted rebar, with failures occurring outside the joint area[4].

Experimental has been conductedon reinforced concrete beams with two types of coupler connections: the tapered coupler and the parallel coupler. The tests revealed a reduction in flexural strength of 3-8% in reinforced concrete beams with either type of coupler splice as compared to beams without such connections, indicating that the inclusion of coupler splice does not result in a significant decrease in performance[5].

In this research, an experiment will be conducted on the utilization of waste rebar steel, which is no longer reusable, as a material for mechanical coupler splice in reinforced concrete beams. The use of waste rebar steel is expected to help save on construction project costs.

2. MATERIAL AND METHODS

2.1 Specimen Details and Parameters

This research tested 3 test specimens of reinforced concrete beams with each having the same size and with the same concrete quality. The difference between the 3 specimens is the rebar splice model dimension. The purpose of the rebar splice placed in the plastic hinge area is to compare the ability of the specimen with the coupler splice and the specimen without the coupler as in Table 1.

Table 1. Types of joints in the RC beams

Number	Specimen	Splice Coupler Model
1	B-13NC	Without Coupler
2	B-13C22W	Coupler Ø19 mm without welding
3	B-13C19	Coupler ø22 mm with welding

The coupler splice is made of waste of rebar with a length of 60 mm and then the pieces of steel rebar are drilled with a diameter of 13 mm, the size of which is adjusted to the rebar that will be given a connection. After the rebar is drilled, a thread is made on the inner surface of the coupler splice and for the steel rebar to be connected, a thread is also given on the outer surface. Details of the coupler splice dimensions can be seen in figure 1.

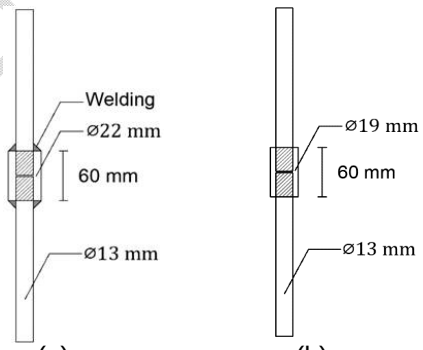

Fig. 1. (a) Coupler splice details on B-13C22W (b) Coupler splice details on B-13C19

The test specimen is a reinforced concrete beam with dimensions of 200 x 300 mm with a height of 1350 mm. The beam uses 13 mm diameter rebar and uses 10 mm rebar. The coupler splices are placed on the plastic hinge beam so as to maximize the ability of the coupler splices. In order for reinforced concrete beams to be tested under cyclic load, a concrete foundation that is directly connected to the beam is required. The reinforced

concrete beam has a foundation with a cross section size of 1200x700 mm with a concrete foundation thickness of 350 mm. Calculation of flexural and shear reinforcement in accordance withstandard test methods[6].Details of reinforcement and dimensions of test objects can be seen in figure 2.

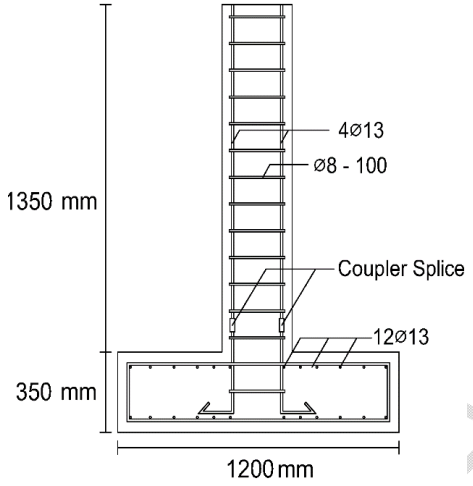

Fig. 2. Rebar details and location of coupler splice on test specimens

2.2 Setup of Test Models

Testing was implemented by applying lateral loads using a cyclic method to determine the capacity of coupler splice under seismic loads. Six anchor points were created on the foundation, where nuts and bolts were installed to secure the specimen to the strong floor, ensuring the test object did not lift during cyclic loading. An actuator with a capacity of 25 tons was used to apply push and pull loads to the beam. The loading point was located at 1100 mm from the bottom end of the beam, as shown in figure 3.

The experiment utilized 5 Linear Variable Differential Transformers (LVDTs) installed horizontally to describe the overall displacement condition of the beam specimen during cyclic loading, and one installed vertically to ensure that the foundation did not lift during the cyclic loading.

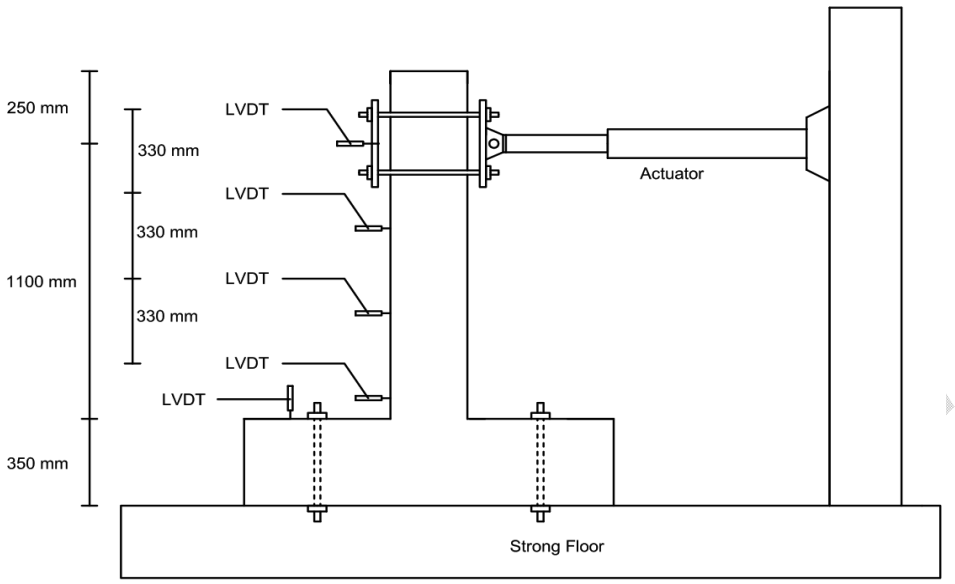

The load application is done gradually and sufficiently slow so that the effects of dynamic inertia and strain rate effects on the material are ignored [7]. The cyclic loading curve can be seen in figure 4. By observing this curve, testing can be conducted by gradually applying push and pull loads with a certain drift ratio. The drift ratio is the ratio between lateral deflection and the height of the lateral load. The drift ratio can be calculated with the following equation below.

$$\text{Drift ratio} = \Delta/L \ (\%) \qquad (1)$$

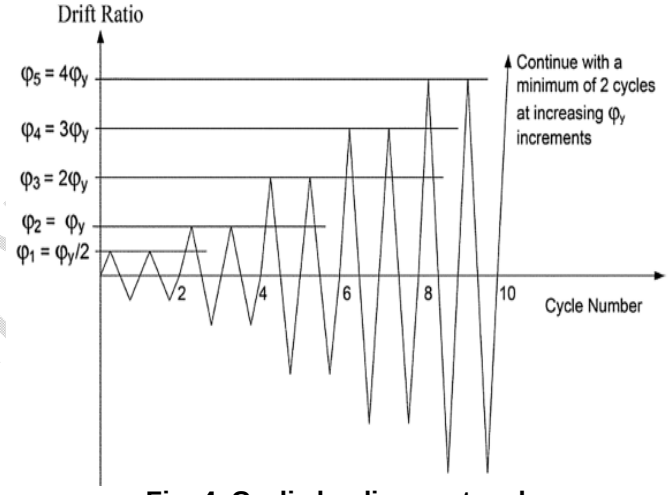

Fig. 4. Cyclic loading protocol

Cyclic loading tests on beam specimens were tested at the structural laboratory, Faculty of Engineering, Gadjah Mada University. Figure 5 is an overview of the test setup.

Fig. 5. Setting of test specimen

3. EXPERIMENTAL RESULTS

3.1 Hysteretic Loops

The hysteretic loops curves of test specimens B-13NC, B-13C22W and B-13C19 which are the ratio between load and displacement of the test results can be seen in figure 6. All loops in the test specimens show ductile behavior in the plastic hinge of the beams, where the structure does not show excessive strength degradation with increasing displacement. The area inside the loops shows that the energy dissipated by the plastic hinge is quite large.

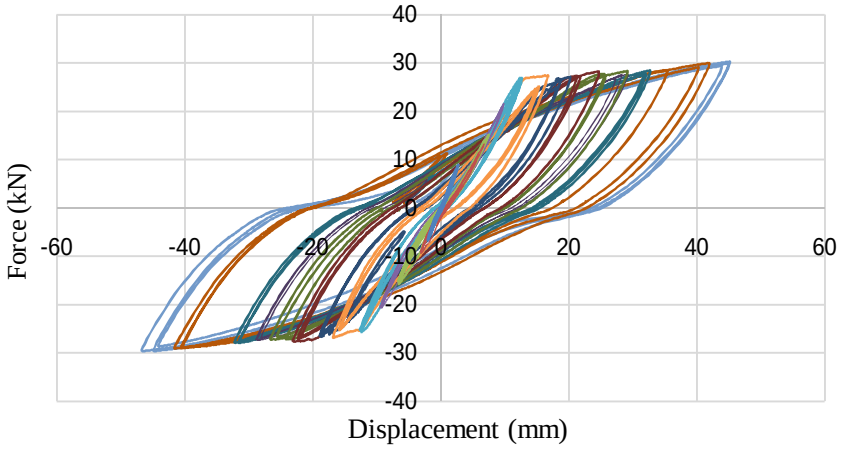

(a) Hysteretic loops curve B-13NC

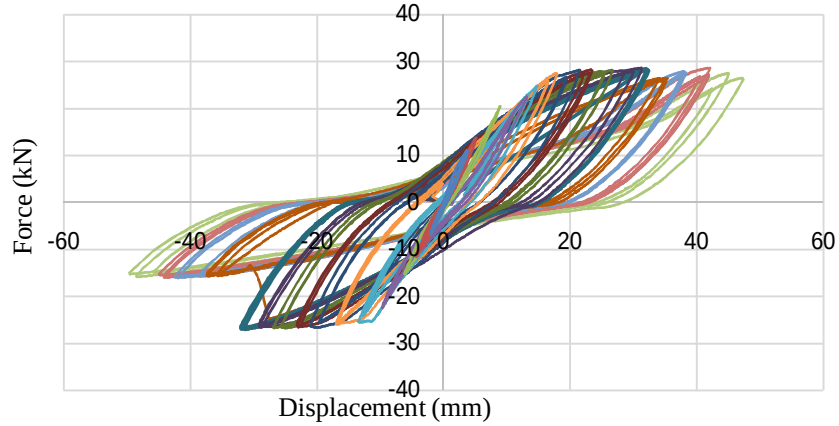

(b) Hysteretic loops curve B-13C22W

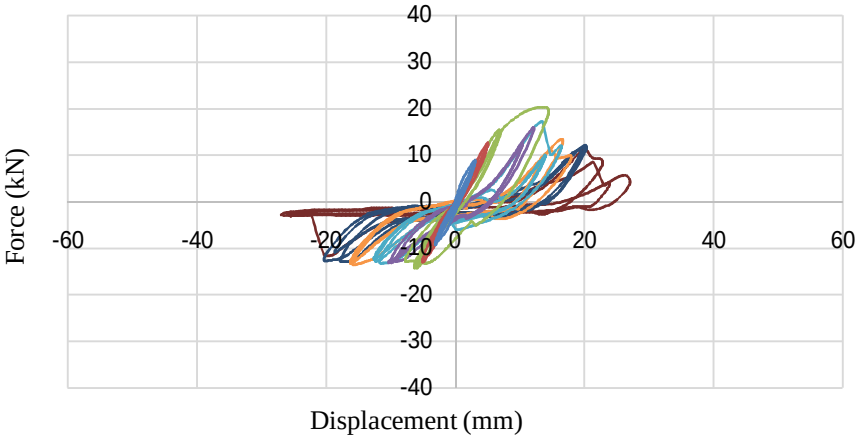

(c) Hysteretic loops curve B-13C19

Fig. 6. Hysteretic loops curve

The maximum load of test specimen B-13NC in the push direction is 30.30 kN with a displacement of 45.17 mm and a drift ratio of 4.11%, while for pull direction loading a maximum load of 29.56 kN is reached with a displacement of 46.76 mm and a drift ratio of 4.25%, Drift ratio is the ratio of displacement to the distance of the load arm (L) 950 mm from the face of the beam. The maximum load of test specimen B-13C22W in the push direction was 28.64 kN with a displacement of 31.28 mm and a drift ratio of 2.84%, while for pull direction loading a maximum load of 26.93 kN was reached with a displacement of 31.98 mm and a drift ratio of 2.91%. The maximum load of test specimen B-13C19 in the push direction was 20.30 kN with a displacement of 14.42 mm and a drift ratio of 1.31%, while for pull direction loading a maximum load of 14.28 kN was reached with a displacement of 7.76 mm and a drift ratio of 0.71%.

3.2 Backbone Curve

Figure 7. shows the backbone curve of specimens B-13NC, B-13C22W and B-13C19 with the load arm 950 mm away from the beam surface. Test specimen B-13NC was able to maintain its strength with a drift ratio exceeding 4% due to push loads and pull loads without experiencing a decrease in strength ≥ 20% of the maximum load. Test specimen B-13C22W was able to maintain its strength with a drift ratio exceeding 4% due to push load without a

decrease in strength ≥ 20% of the maximum load. However, it failed under pull load at drift ratio = 3.85% which resulted in a significant decrease in strength. Test specimen B-13C19 could not maintain its strength with a drift ratio exceeding 4%. A significant decrease in strength due to push and pull loads ≥ 20% of the maximum load occurred before the drift ratio had not reached 3%.

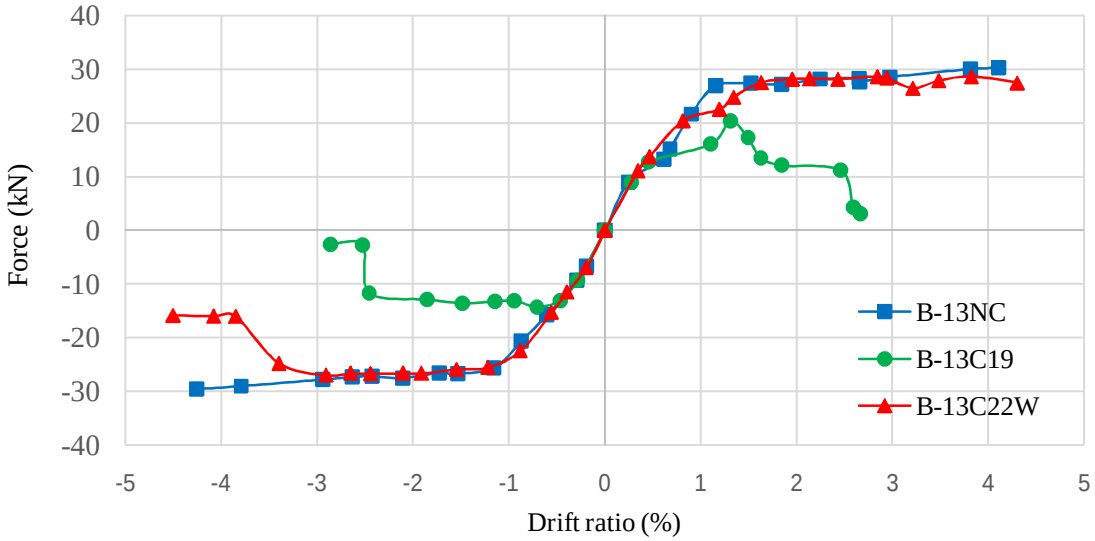

Fig. 7. Backbone curve

3.3Equivalent viscous damping ratio (EVDR)

The effectiveness of the damping force will depend on the duration of the loading, even though the structure has a high damping ratio but at a relatively short loading [8]. Effective damping will then greatly reduce or eliminate sway. The Equivalent Viscous Damping Ratio (EVDR) can be calculated based on the equation below.

$$\mathbf{EVDR} = \frac{\mathbf{HE}}{\mathbf{2.\pi.PE}}$$

HE value is hysteretic energy and PE is potential energy. The maximum EVDR values in specimens B-13NC, B-13C22W and B-13C19 are 17.52%, 18.92% and 33.64%, respectively. Test specimens B-13NC and B-13C22W have relatively similar characteristics of gradual increase in EVDR while test specimen B-13C22W experienced significant increase in EVDR compared to other test specimen.

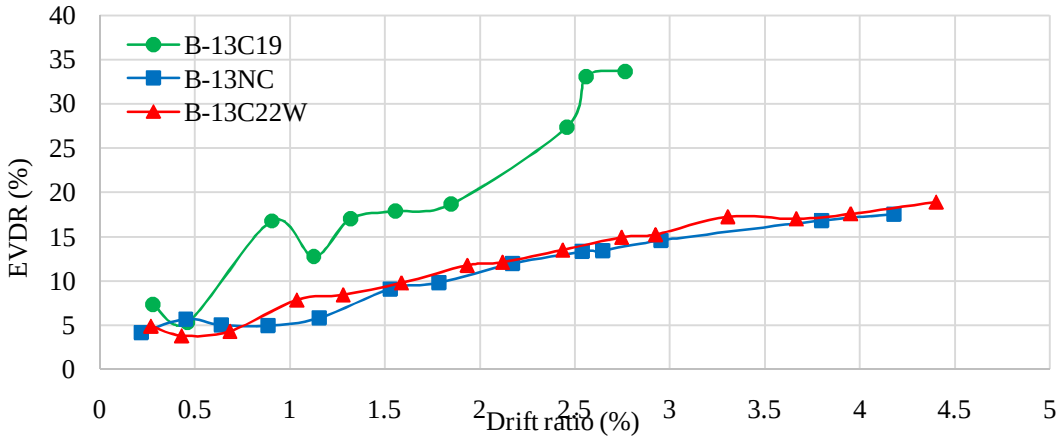

Fig. 8. EVDR curve

3.4Stiffness

Stiffness is defined as the force required to cause a deflection. The stiffness value is the angle of inclination of the relationship between load and deflection[9]. The stiffer the structure, the greater the stiffness value. Figure 9. illustrates that the first cycle stiffness of test specimens B-13NC, B-13C22W and B-13C19, as the drift ratio increases, it can be seen that the stiffness decreases, which is due to cracks in the concrete, reinforcement slip, melting of the reinforcement and spalling.

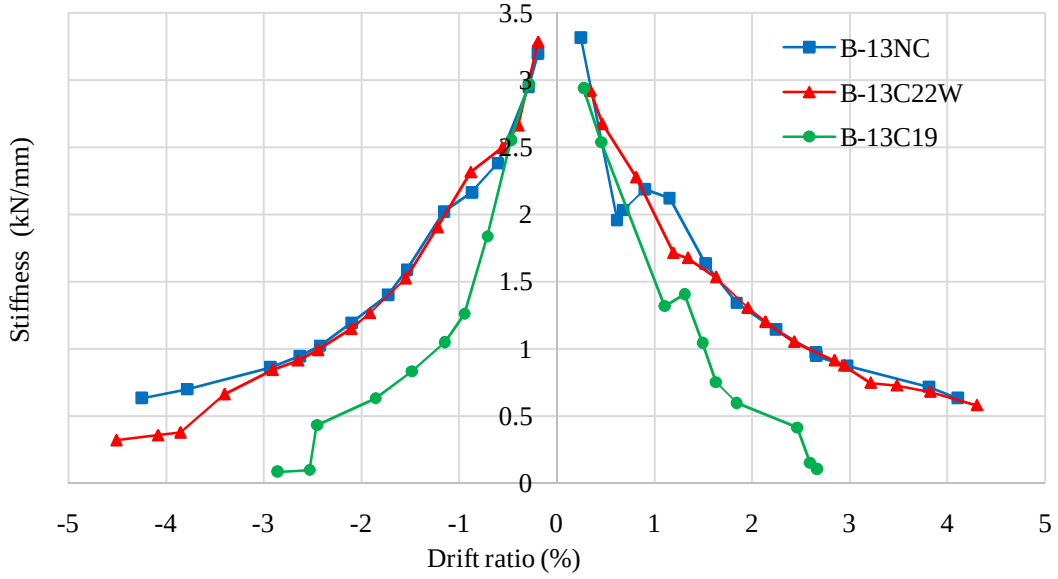

Fig. 9. Stiffness value of test specimen

The average stiffness of the B-13NC and B-13C22W test specimens at a drift ratio of 4% was 0.75 kN/mm and 0.71 kN/mm, respectively. Test specimens B-13NC and B-13C22W have almost the same stiffness value, which indicates that the addition of a 22 mm diameter coupler splice to test specimen B-13C22W does not affect the stiffness value of the structure. While the stiffness of the pull load, the B-13C22W test specimen experienced a significant decrease due to the failure of one of the splices. For test specimen B-13C19, the coupler splice has failed before the drift ratio reaches 2.5% so that the stiffness value of test specimen B-13C19 is very small due to push and pull loads.

Table 2. Stiffness of test specimen

Test Specimen	Drift Ratio (%)	Stiffness (kN/mm)			Stiffness Percentage (%)
		Push	Pull	Average	
B-13NC	4	0,75	0,71	0,73	22,29
B-13C22W	4	0,71	0,50	0,60	19,70
B-13C19	2,5	0,47	0,49	0,48	16,27
Average				0,60	19,42

From Table 2, it can be seen that the percentage of stiffness of test specimens B-13NC and B-13C22W at a drift ratio of 4% is 22.29% and 19.70% of the initial stiffness, respectively, while the percentage of stiffness for test specimen B-13C19 at a drift ratio of 2.5% is 16.27%. The comparison of the percentage of stiffness of the specimens can be seen in figure 10.

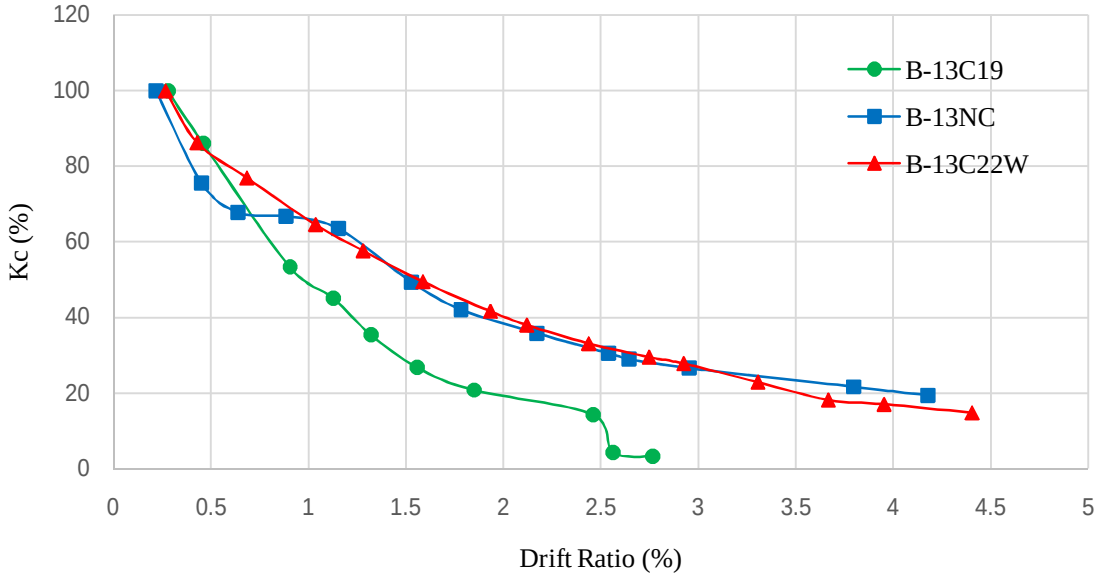

Fig.10. Percentage stiffness of test specimens

3.5Ductility

Ductility is the ability of a structure to avoid rapid collapse[10].The ductility value of the structure is based on the results of the equivalent elastic plastic curve (EEPC) analysis to obtain the relationship between load and displacement at the first crack, yield, peak, and failure conditions. Figure 10. and figure 11. show the EEPC of specimens B-13C22W and B-13C19, respectively.figure 11. describes the EEPC curve of specimen B-13C22W. From the curve The displacement value of a structure can be obtained when experiencing yield, peak and failure conditions so that the ductility value of the structure can be calculated. Test

specimen B-13C22W has a ductility value due to push load of 3.93 while for ductility due to pull load of 3.46. B-13C19 has a ductility value 2.92 due to push load, while the ductility due to pull load is 2.44. The EEPC curve for B-13C19 can be seen in figure 12.

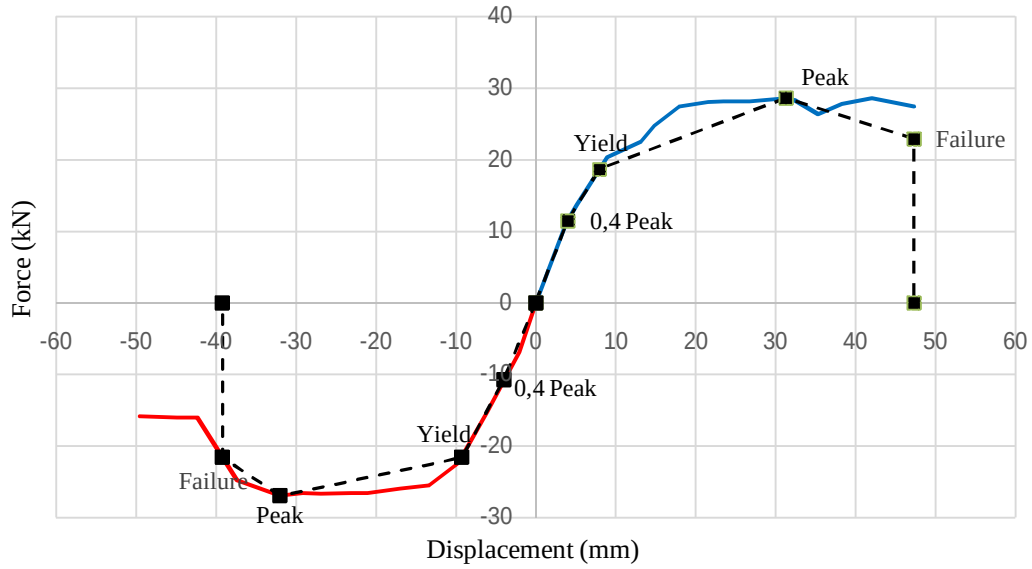

Fig. 11. EEPC of B-13C22W

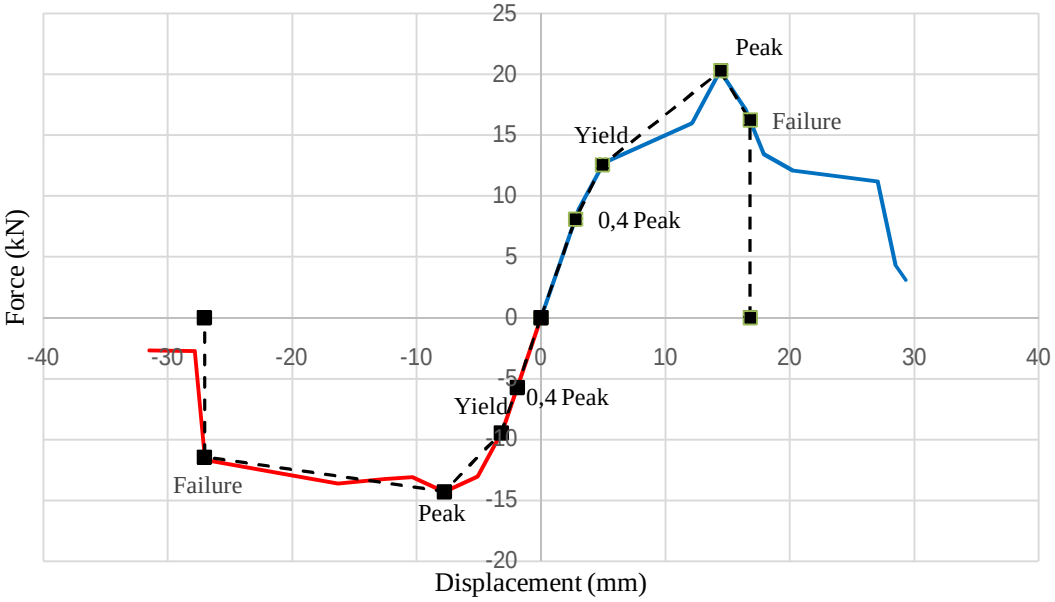

Fig. 12. EEPC of B-13C19

3.6Collapse Mechanism

From the experimental result of test specimen B-13C22W, a failure of steel rebars occurred in the plastic hinge area of the beam which resulted in a decrease in the strength of the test specimen beam due to pull direction loading. The failure occurred when the specimen

received a pull direction load at the 11th cycle of 26.93 kN. The rebar failure occurred at the welding at the coupler ends. Details of the failure of the rebar can be seen in figure 13.

(a) (b)

Fig. 13. (a) Failure location of steel rebar (b) Detail failure condition of steel rebar.

Tests on test specimen B-13C19 also had a failure of the structure in the area of the plastic hinge of the beam. Unlike test specimen B-13C22W which only failed one coupler splice, test specimen B-13C19 had two failure of coupler splice during push direction loading with a strength of 20.30 kN and pull direction loading with a strength of 14.28 kN. Failure of both coupler splice was caused by detachment of the rebar from the 19 mm diameter coupler splice. Details of the failure of the rebar can be seen in figure 14.

(a) **(b)**

Fig. 14. (a) Failure at steel rebar thread (b) Steel rebar detached from coupler

4. CONCLUSION

Based on the test results on the coupler splice on reinforced concrete beams in the plastic hinge area, several conclusions can be concluded :

1. Based on the damage pattern that occurs in the test specimens B-13NC, B-13C22W and B-13C19 shows the occurrence of flexural failure. The flexural failure mechanism is fulfilled by starting the flexural failure until the longitudinal rebar yields before shear failure and yielding of shear rebar.

2. From the hysteretic loops curve, it shows that with the installation of the coupler splice on the B-13C22W specimen, it has a maximum strength of 28.64 kN, which is almost the same as the maximum strength of the specimen without connection of 30.30 kN. However, specimen B-13C19 has a strength of 20.30 kN which is far below that of specimens B-13NC and B-13C22W.

3. The coupler splice on B-13C22W has almost the same energy dissipation ability as the test specimen without connection (B-13NC) when receiving a push load but has decreased energy dissipation ability due to pull load when the drift ratio is less than 3.5% due to the failure of the splice. B-13C19 had a failure at the coupler splice due to both push and pull loads which resulted in the specimen having a much lower energy dissipation capability than the other specimens.

4. The ductility of the B-13C22W specimen has an average value of 3.69 while the B-13C19 specimen has an average ductility value of 2.68. Test specimen B-13NC has an average ductility value of 5.46 so that the coupler splice at the plastic hinge reduces the ductility ability of the structure.

5. The stiffness of the structure of test specimens B-13NC, B-13C22W and B-13C19 decreased along with the increase in drift ratio. test specimens B-13NC and B-13C22W have almost the same value of decreasing stiffness gradually, but B-13C19 has a considerable decrease in stiffness compared to other test specimens.

REFERENCES

1. Dipohusodo I.Reinforced Concrete Structure. Jakarta: Gramedia; 1994
2. Wahyudi L. Standard reinforced concrete structureSNI T-15-1991-03.Jakarta: Gramedia; 1991
3. Negara JB. Analysis of Waste Rebar Materials in Building Construction Projects. Journal ofCivil Engineering. 2019:1–11.
4. Kruavit P, Ruangrassamee A, Hussain Q. Experimental and analytical study on reinforcing steels with threaded mechanical couplers under monotonic and cyclic loadings. Engineering Journal. 2020;24:61–70.
5. Jeong JH, Kim IT. LeeMJ, Ahn JH. Mechanical Performance Evaluation of Rolling Thread Steel Rebar Connection with Taper type Coupler. Journal of the Korea institute for structural maintenance and inspection.2015:40–51.
6. National Standardization Organization.SNI 2847-2019: Structural Concrete Requirements for Buildings and Explanations. Jakarta;2019.
7. ACI 374.2R-13.Guide for Testing Reinforced Concrete Structural Elements under Slowly Applied Simulated Seismic Loads. 2013.

8. Mutawalli M. Stability of Smart frame Type T light steel structure connection against Cyclic Load in Simple Earthquake Resistant House Building Knock Down System.Department of Civil and Environmental Engineering.2007
9. Gere JM, TimosenkoSP. Mechanics of Materials. Jakarta: Gramedia; 2007
10. Park R, PaulayT. Reinforced Concrete Structure, NewYork: A Wiley Interscince Publication; 1994

:

APPENDIX